This article has been accepted for publication in a future issue of this journal, but has not been fully edited. Content may change prior to final publication. Citation information: DOI 10.1109/TIE.2014.2361114, IEEE Transactions on Industrial Electronics

Induction Machine Insulation Health State Monitoring Based on Online Switching Transient Exploitation

Peter Nussbaumer, *Member, IEEE,* Markus A. Vogelsberger, Thomas M. Wolbank, *Member, IEEE*

***Abstract*--Today's variable speed drives are usually operated close to their maximum tolerable conditions. The fast switching of modern power electronic devices leads to high stress of the winding insulation. As a result, an insulation breakdown may lead to sudden breakdown and high economic loss. To avoid unpredictable downtimes and enable repair on demand, monitoring of insulation health state is getting more and more important.**

The paper proposes a method to monitor changes in the insulation health state by evaluating the machines high frequency properties. Deterioration of insulation condition is usually linked with a change of insulation capacity and thus also influences high frequency properties. Initiating a voltage step excitation of the machine by the switching of the inverter, the high frequency properties can be identified by measuring the resulting current response. This response is usually seen as current signal ringing and contains the machines high frequency information.

Applying signal processing tools changes in the high frequency information is extracted and an insulation state indicator derived. The applicability of the method is verified by measurements on two test machines (5.5kW and 1.4MW) having different power rating as well as different insulation system.

***Index Terms*--AC machines, Condition monitoring, Electric machines, Fault diagnosis, Induction motors, Insulation testing, Motor drives, Pulse width modulated inverters, Rotating machines, Squirrel cage motors**

NOMENCLATURE

C	Capacitance.
f	Frequency.
f_S	Sampling frequency.
g	Discrete frequency.
i	Current.
ISI	Insulation state indicator.
k	Identifier of consecutive measurement.
m	Number of measurement repetitions.
N	Number of samples.
n_{high}	Higher limit of frequency range.
n_{low}	Lower limit of frequency range.
R	Resistance.
$RMSD$	Root mean square deviation.
$SISI$	Spatial insulation state indicator.
t	Time.
t_{win}	Time window length.
U_{DC}	DC-link voltage.
x_1	Signal 1.
x_2	Signal 2.
y	Current with eliminated derivative.
Y_{con}	Fourier transformed of condition measurement.
Y_{ref}	Fourier transformed of reference measurement.

Subscripts

c	Cable.
c-c	Cable-to-cable.
fault	Fault.
p, ph	Phase.
ph-gnd	Phase-to-ground.
ph-ph	Phase-to-phase.
t-t	Turn-to-turn.
U,V,W	Machine phase.

Manuscript received January 30, 2014; revised May 27, 2014 and July 10, 2014; accepted July 29, 2014.

P. Nussbaumer was with the Institute of Energy Systems and Electrical Drives, Vienna University of Technology, 1040 Vienna, Austria. He is now with Bombardier Transportation (Switzerland) Ltd., Converter Control Department GSC/NE2EP, 8050 Zurich, Switzerland (e-mail: peter.nussbaumer@ch.transport.bombardier.com)

M. A. Vogelsberger is with Bombardier Transportation Austria GmbH, GSC/NDEW; PPC-Drives Development Center 1, 1220 Vienna, Austria (e-mail: markus.vogelsberger@at.transport.bombardier.com)

T. M. Wolbank is with the Institute of Energy Systems and Electrical Drives, Vienna University of Technology, 1040 Vienna, Austria (phone: +43 (1) 58801 - 370 226; fax: +43 (1) 58801 - 9370 226; e-mail: thomas.wolbank@tuwien.ac.at).

I. INTRODUCTION

IN modern traction application adjustable speed drives (ASD) consisting of an AC machine (typically induction or permanent magnet synchronous (PMSM) machine) and inverters (nowadays voltage source inverters (VSI) with Insulated Gate Bipolar Transistors (IGBTs) are standard. Although electrical machines are generally highly reliable, the increased demand of system availability leads to the necessity to implement condition monitoring, fault detection and/or fault tolerant control.

The main causes for machine breakdown have been analyzed in [1] and [2]. The outcome of this analysis is that machine breakdown originates in faults that can be classified in three categories – bearing, stator and rotor related faults. According to these investigations the second most common causes are stator related accounting for about 35% of all collected machine breakdowns. Within these stator related faults, problems with the insulation finally leading to short circuit faults account for 70%. Thus, reliable monitoring of the insulation condition allows the shift of maintenance strategy from preventive to predictive. In case of predictive maintenance, the risk of failure estimated by insulation condition monitoring allows to decide if maintenance (e.g. replacement of the windings before breakdown of the insulation system) is required or not. In the past, different fault detection and condition monitoring techniques have been presented. In [3] and [4] many condition monitoring and fault diagnosis methods have been summarized. Further studies presented in [5] and more recent in [6] discuss the development of online monitoring methods of the machine's winding insulation.

Usually breakdown of the insulation is a slowly developing process starting with deterioration of the

This article has been accepted for publication in a future issue of this journal, but has not been fully edited. Content may change prior to final publication. Citation information: DOI 10.1109/TIE.2014.2361114, IEEE Transactions on Industrial Electronics

insulation material and then leading to severe turn-to-turn, phase-to-phase or phase-to-ground short circuits [8]. The exact time of insulation breakdown cannot be determined according to [9]. Therefore only a risk of failure rather than a time to failure can be defined.

The deterioration of the insulation condition is accelerated by different causes. The main cause according to [10] is thermal stress. However, electrical, mechanical and environmental strains lead to deterioration of the insulation material too. Concerning inverter-fed drives the fast rise times of modern switching devices like IGBTs and MOSFETs lead to increased electrical stress for the insulation system as analyzed in [8]. This aspect of accelerated insulation aging due to PWM (Pulse Width Modulated) inverter operation has been discussed in many publications so far. To further investigate these effects modeling of the behavior of electrical machines in case of fast voltage switching has been realized. The results in [11],[12] show that the electrical stress due to the high rate of voltage rise in case of PWM inverter operation influences the life time of the insulation material. However, the experimental results show that the magnitude of the applied voltage and the temperature are influencing the life time more than the frequency of the applied voltage (switching frequency in case of inverter-fed operation). The dependence of electrical stress (high dv/dt) on the cables and the relationship between partial discharges and insulation life time is discussed in [13].

So far, many different insulation fault detection and condition monitoring techniques have been proposed in literature. All methods can be categorized into offline or online approaches. The most industrially accepted methods are applied offline. Thus, the machine has to be taken out of service to test its insulation. Furthermore, it can be differentiated if the tests are able to detect insulation deterioration or solid short circuits only.

Some of the proposed methods use artificial neural networks to detect solid short circuits in the stator windings with various inputs like presented in [14], [15] and [16]. The comparison of the estimated back EMF (electro-motive force) to reference measurements is used in [17] and [18]. The detection of inter-turn short circuits for claw-pole machines is presented in [19]. The method uses a machine model to detect the effects of turn short circuits in the DC-link quantities due to the lack of measurements on the AC side. This method could be also applicable for poly-phase machines. In [20] and [21] on the other hand the analysis of the negative sequence components is used for insulation fault detection. The comparison of the second order harmonics in the quadrature current component to measurements at faultless condition for inter-turn short circuit detection in permanent magnet synchronous machines (PMSM) is used in [22].

The offline partial discharge [6],[7] and offline surge [23] tests are able to detect insulation deterioration. Further offline insulation monitoring methods are the DC conductivity test [24], the insulation resistance (IR) test [9], DC/AC HiPot test [9] and polarization index (PI) test [9].

So far, the only industrially accepted online insulation monitoring technique is the online partial discharge (PD) test [25] that has been discussed more recently in [26], [27] and [28]. However, this test is only applicable for medium to high voltage machines and needs additional measurement hardware as well as highly sophisticated evaluation software. Different other online insulation fault detection methods have been presented in literature.

The on-line capacitance and dissipation factor test is discussed in [29] for monitoring of the insulation condition. Furthermore, the estimation of the leakage current to ground is used to assess the condition of the ground-wall insulation by measuring the current in all three phases. The investigation of the capacitance and dissipation test and analysis of other insulation condition monitoring techniques are also presented in [30] and [31]. There the leakage current to ground is used for assessment of the ground wall insulation condition. However, in this case the current in all three phases is measured with only one single current transducer resulting in a direct estimation of the leakage current.

The adaptation of the surge test for online applicability is proposed in [32] and [33]. So far, this test is designed for application in mains-fed machines only.

All of the above presented methods have a certain disadvantage. This can be the need of additional sensors or high sophisticated evaluation leading to high computational effort or the lack of possibility to detect incipient stator insulation degradation. Furthermore, many methods only work for mains-fed operation or only if the machine under test has been taken out of operation. The insulation monitoring method that will be presented in the following aims to overcome these disadvantages. Thus, the requirements for the proposed online insulation monitoring method are applicability for inverter-fed drives, usage of the already available sensors only, the detection of insulation deterioration and that no disassembling of the drive is necessary.

First results on exploitation of switching transients to insulation state monitoring have been presented in [34], however, most of the results are limited to low power machines with random wound stator windings and enamel-insulated wire.

This paper briefly presents the developed online insulation monitoring method and compares its application to two different induction machine drive systems with different winding type as well as insulation system and power rating. Special focus is laid on the high power, high voltage insulation system. Furthermore, the performance of the method for different sampling rates for the current measurements is analyzed.

II. Theoretical Description of Proposed Monitoring Method

A. *High-Frequency Behavior of Inverter-Fed Drives*

The fast voltage rise time of modern switching devices additionally stresses the winding insulation as mentioned in the introduction. The reason for this stress is the occurring transient overvoltage resulting from reflections of the applied voltage pulse at the machine's terminal connections. According to traveling wave theory the mismatch of machine and supply cable impedance leads to these reflections [35]. The machine impedance is by far bigger than the cable impedance. Thus, in theory the voltage pulse is fully reflected (reflection coefficient nearly one) [35]. The reflected voltage pulse leads to an oscillating transient

This article has been accepted for publication in a future issue of this journal, but has not been fully edited. Content may change prior to final publication. Citation information: DOI 10.1109/TIE.2014.2361114, IEEE Transactions on Industrial Electronics

overvoltage with decaying magnitude. The peak value can reach up to twice or even four times (for fast subsequent voltage pulses) the DC-link voltage and the oscillation frequency is in the range of tens kHz to tens MHz [36].

An inverter-fed drive system consists of three main components defining the complex impedance system leading to the voltage pulse reflections:

- Inverter (e.g. voltage source inverter)
- Supply cables
- AC machine (e.g. induction machine)

The elements defining the characteristic of the drive's behavior like stator resistance r_S, stator inductance l_S, cable inductance and resistance per unit length, etc. on the one hand and the parasitic components like phase-to-ground (cable), winding-to-ground (machine), winding-to-winding (machine) and turn-to-turn (machine) capacitance and the inverter's capacitive coupling to ground on the other hand determine the mentioned drive's complex impedance network. Many of the parasitic components are defined and strongly influenced by the insulation system. Thus, these components also influence the oscillating transient voltage. This oscillation is also visible in the current immediately after inverter switching. It is characteristic for the machine's high-frequency behavior.

A change in the machine's insulation system (e.g. due to deterioration) leads to a change in this characteristic oscillation (hf-behavior). The proposed condition monitoring method evaluates the oscillation in the current reaction on voltage switching to detect changes in the machine's hf-behavior. It is preferred to analyze the changes in the current oscillation as current sensors are already available in modern drive systems for machine control.

There are also other influences that lead to changes in the drive system's high-frequency behavior. On the one hand change of cabling could lead to changed hf-behavior. However, as investigated in [37] this does not affect the proposed method. On the other side environmental conditions like temperature or moisture can cause a change of the machine's hf-behavior. Experimental investigations showed that this does not significantly influence the methods performance. Atmospheric pressure variation is not an issue for this monitoring technique. In the relevant standards EN60216-1 up to 8, IEEE 429, EN60172 and EN60212 dealing with insulation testing no hint can be found that atmospheric pressure variation has to be taken into account. Furthermore, the application is aiming on operation close to normal pressure.

B. Measurement Procedure and Signal Processing

For the evaluation of the hf-oscillation the current has to be acquired with sufficient resolution in time. The excitation of the machine in the hf-range is carried out by changing the inverter's switching state.

The used switching state transitions always originate in the lower short circuit (-SC, 000) and end in one of the three positive active switching states (+U, 001; +V, 010; +W, 100). For the generation of these switching transitions and thus applied active voltage states the VSI of the drive system is used. Thus, it is not necessary to take the drive out of service and no additional hardware is needed.

The current's reaction resulting from the switching transition in phase U (-SC to +U) is depicted in Fig. 1. Although this reaction contains frequency components above the bandwidth of industrial current sensors (bandwidth between several ten to a few hundred kHz) no special sensors are necessary. Standard industrial current sensors do not have a sharp cut-off characteristic but only lead to attenuation of the frequency components above their specified frequency. The current sensors used in these investigations have a cut-off frequency of 300kHz (Vaccuumschmelze ZKB 464/201).

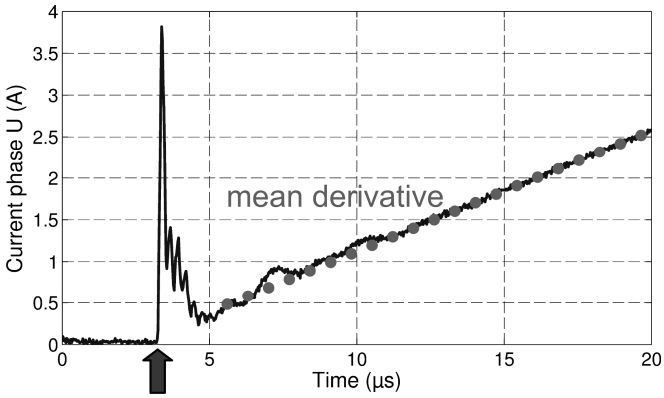

Fig. 1. Current signal with illustrated mean derivative (dotted line) and switching instant (arrow).

The visible current derivative after the switching transition (denoted "mean derivative" – dotted line) is mainly determined by the machine's transient leakage inductance. This transient leakage inductance depends on inherent machine saliencies like rotor slotting and saturation level. Thus, this influence has to be eliminated as only the high-frequency oscillation is of interest. The elimination can be done by simply subtracting the mean derivative after exact detection of the actual switching instant. For the calculation of the mean derivative two current samples $i(t_1)$ and $i(t_2)$ at steady state current derivative are needed. For the trace depicted in Fig. 1 t_1 and t_2 could be chosen to 13µs and 18µs. The elimination of the current derivative is then done as follows.

$$y(t) = i(t) - \frac{i(t_2) - i(t_1)}{t_2 - t_1} \cdot t \qquad (1)$$

The resulting signal is shown in Fig. 2.

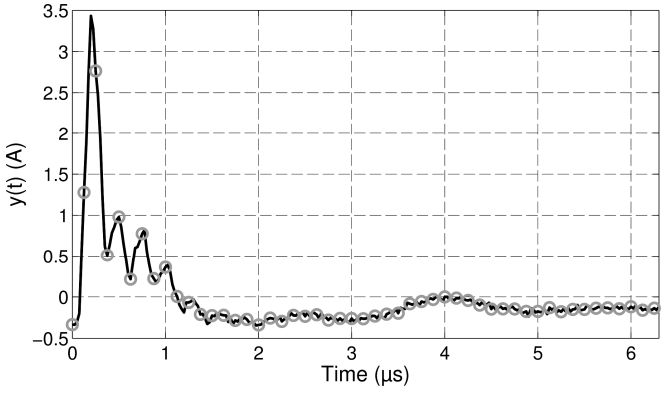

Fig. 2. Current (mean derivative subtracted) after switching transition from lower short circuit (-SC, 000) to +U (001).

The time instant of the switching command is used as a pre-trigger for the detection of the exact switching instant. Thus, the data collection starts before the actual switching instant. After data acquisition the trigger detection can be

This article has been accepted for publication in a future issue of this journal, but has not been fully edited. Content may change prior to final publication. Citation information: DOI 10.1109/TIE.2014.2361114, IEEE Transactions on Industrial Electronics

performed by taking the difference between two subsequent samples for several combinations of samples. If the differences of these samples exceed a certain threshold the actual position of the switching transition is found. If not another set of differences is calculated for later samples. This procedure is repeated until the actual switching transition has been identified. The whole algorithm consists of subtractions and comparisons only. Hence, it can be easily implemented in a FPGA or DSP (Digital Signal Processor).

The circles only highlight exemplary sampling instants for better illustration and do not reflect the actual used maximum sampling rate of 40MS/s. The transient current oscillation depicted above is further analyzed in the frequency domain. Therefore the depicted signal is transformed by Fast Fourier Transform (FFT). The investigated time window is chosen from the actual switching instant until the oscillation has decayed. For the shown signal (Fig. 2) this time window is chosen to 6.4µs. The used sampling frequency is 40MS/s. Thus, the number of sample values equals to *N=256*. The resulting amplitude spectrum after Fourier transform is depicted in Fig. 3 for evaluation in phase U.

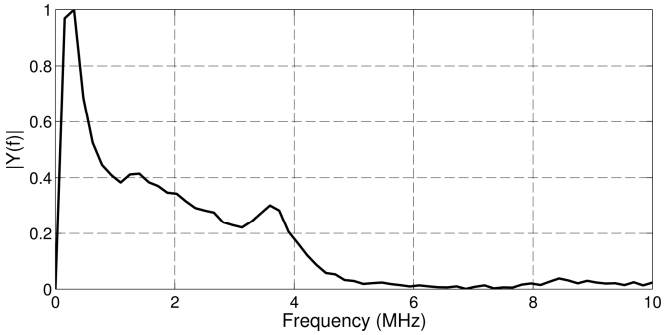

Fig. 3. Amplitude spectrum of measured current in phase U after switching transition from lower short circuit (-SC, 000) to +U (001).

The amplitude spectrum is characteristic for the machine's hf-behavior in phase U. If recorded for healthy machine condition it serves as a reference trace and is compared to later measurements to assess the machine's insulation condition in the proposed monitoring method. It is important to compare traces at same operating condition. Currently the method is based on evaluation of measurements for unexcited machine.

To detect changes in the machine's hf-behavior the above described measurement procedure and signal processing is repeated for all three phases. For each of the three phases a reference amplitude spectrum (recorded for healthy machine condition) is stored for later comparison to condition measurements and assessment of the insulation condition.

C. Insulation State Indicator (ISI/SISI)

The measurement and signal processing has been described in the previous section. The next step is to introduce an insulation state indicator for the assessment of the insulation condition in one phase. It is based on quantifying the change in the machine's high-frequency behavior by comparison of amplitude spectra recorded for healthy machine condition (reference) and that recorded during later condition assessment. The Root Mean Square Deviation (RMSD) is chosen as a comparative value and serves as Insulation State Indicator (ISI) for the respective phase.

$$ISI_{p,k} = RMSD_{p,k}(x_1, x_2) = \frac{\sqrt{\sum_{g=n_{low}}^{n_{high}} \left(Y_{ref,p}(g) - \left|Y_{con,p,k}(g)\right|\right)^2}}{n_{high} - n_{low}} \quad (2)$$

The Fourier transformed signals Y_{ref} and Y_{con} have been obtained by the procedure described in section B. for healthy machine condition (reference) and a later condition assessment, respectively. The index p defines the investigated phase (U,V,W). The variables n_{high} and n_{low} define the compared frequency range and depend on sampling rate and investigated window length. The definition of the evaluated frequency range allows separating other influences like cabling or grounding that is also leading to a change in the drive's high-frequency behavior. Due to the fact that a single measurement's duration is in the range of hundred microseconds the procedure can be repeated *m*-times to increase the accuracy of the method. Thus, the index k (1,2,3,…) denotes the number of the consecutive measurements. Investigations showed that 30 repetitions of the measurements are more than sufficient for a robust detection. This outcome also correlates with the fact that a statistically representative sample is greater or equal to 30 if the measurand is normally distributed as can be assumed here.

The used reference signal (frequency spectrum for healthy machine condition) is the mean trace calculated from *m* measurements.

$$Y_{ref}(g) = \frac{\sum_{k=1}^{m} \left|Y_{ref,k}(g)\right|}{m} \quad (3)$$

The variable g identifies the discrete frequency. The frequency is calculated using the sampling rate f_S, the number of samples N and the window length t_{win} according to the following equation

$$f = \frac{g \cdot f_s}{N};\ g = 0,1,2,3,...;\ N = t_{win} \cdot f_s\,. \quad (4)$$

The quantity defining the insulation condition in one phase is the insulation state indicator ISI_p calculated from *m* RMSD values according to equation (2).

$$ISI_p = \frac{\sum_{k=1}^{m} ISI_{p,k}}{m} \quad (5)$$

In a last step of signal processing a Spatial Insulation State Indicator (SISI) is calculated by linear combination of the ISI values of all three phases.

$$SISI = ISI_U + ISI_V \cdot e^{j\frac{2\pi}{3}} + ISI_W \cdot e^{j\frac{4\pi}{3}} \quad (6)$$

Symmetrical changes of the high-frequency behavior (e.g. due to temperature variation, change of cabling,…) are eliminated by this linear combination as these lead to a zero-sequence component.

It has to be stressed here that the method is aiming on insulation condition monitoring and not on fault detection of already occurred short circuits in the machine winding. Accelerated insulation aging due to increased stress is still a slow process. The focus of this method is not on detecting suddenly occurring insulation faults but observing a trend of the insulation state indicator over time. This trend can then be used for an assessment of the insulation condition and as

This article has been accepted for publication in a future issue of this journal, but has not been fully edited. Content may change prior to final publication. Citation information: DOI 10.1109/TIE.2014.2361114, IEEE Transactions on Industrial Electronics

an indicator for incipient insulation deterioration. Hence outliers can be eliminated easily leading to a low risk of false alarms.

III. Experimental Setup

The main focus in this paper is to show the applicability of the above proposed condition monitoring method to machines with high power rating and detect the necessary sampling rates for the current measurements. Furthermore, results are compared for induction machines that clearly differ in their power rating as well as the used insulation systems. Two different machines have been chosen for this purpose. Induction machine IM#1 is an industrial 2-pole machine with 5.5kW (low power; see Appendix) and enamel-insulated wire and random wound coils. Induction machine IM#2 on the other hand is a 4-pole 1.4MW machine (high power for traction applications; see Appendix) with fiber-insulation wires and pre-formed coils. Both machines have a squirrel cage rotor and several tapped windings accessible at the machine's terminal connection block. Thus, it is possible to change the machine's hf-behavior by inserting capacitors between the different taps of the winding. The exemplary scheme of the parasitic capacitances (phase C_{ph}, turn-to-turn $C_{t\text{-}t}$, phase-to-phase $C_{ph\text{-}ph}$, phase-to-ground $C_{ph\text{-}gnd}$) in the machine and this additional capacitor C_{fault} are depicted in Fig. 4.

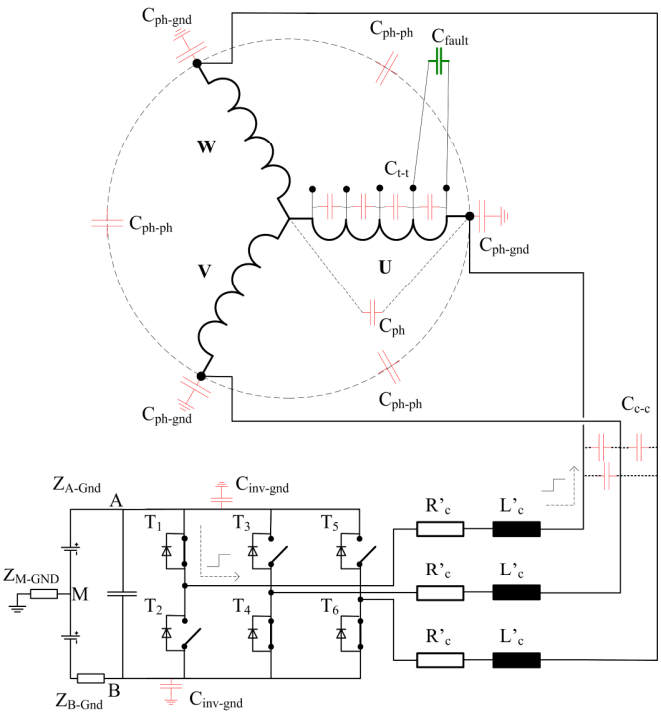

Fig. 4. Additional capacitor C_{fault} inserted in parallel to the full phase winding U, schematically.

The phase-to-ground capacitances of IM#1 and IM#2 are 1.5nF and 21nF respectively. The additional capacitor in parallel to the turn-to-turn capacitances, thus, result in an increase of the insulation capacitance. Due to the fact that aged insulation material would lead to a similar increase of capacitance this approach is chosen to emulate insulation deterioration. The severity of insulation degradation can be varied by the capacitance of the inserted capacitor. This is in accordance to the results of increasing capacitance due to insulation deterioration presented in [38] and [39]. In these investigations the turn-to-turn insulation is thermally aged at 250°C. The thermal aging leads to an increase of capacitance of up to twice the initial value. It is thus expected that the accuracy reached is sufficient to detect incipient insulation fault. Furthermore, the severity of insulation deterioration can be varied by location of the insertion of the capacitor. In these investigations the capacitor is inserted in parallel to the winding of one whole phase (denoted as 'full'; winding consists of 12 coils), one coil (consisting of 5 turns) and one turn. IM#1 and IM#2 have the same winding configuration.

The used test-stand is schematically depicted in Fig. 5. Fig. 6 shows a picture of the used laboratory test-stand. The machines under test IM#1 (low power) and IM#2 (high power) are connected to an IGBT-voltage source inverter fed by a relatively constant DC-link voltage of 440V.

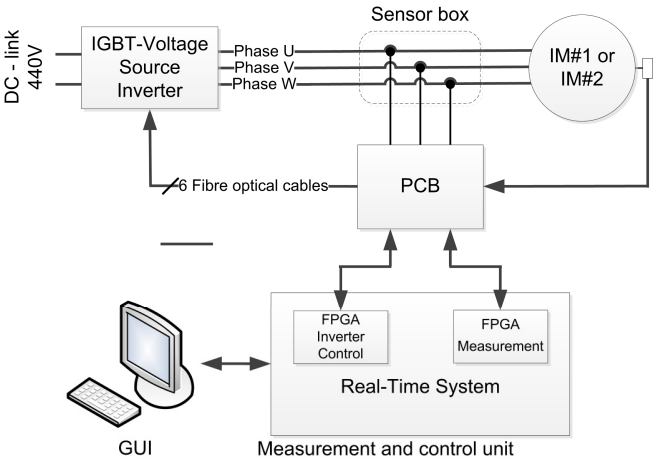

Fig. 5. Schematic overview of used test-stand.

The measurements, control and signal processing are carried out with a combined PXI-system consisting of real-time processor, Field Programmable Gate Array (FPGA) and fast sampling ADCs from National Instruments, programmable in LabVIEW. The inputs and outputs of the real time system and FPGA are connected to a printed circuit board (PCB). The interfaces and signal adaption of sensors and gate drive unit control signals are realized on this PCB. Control and gate drive unit are connected via fiber optical cables. The user interface for the control system is realized on a conventional PC connected via Ethernet.

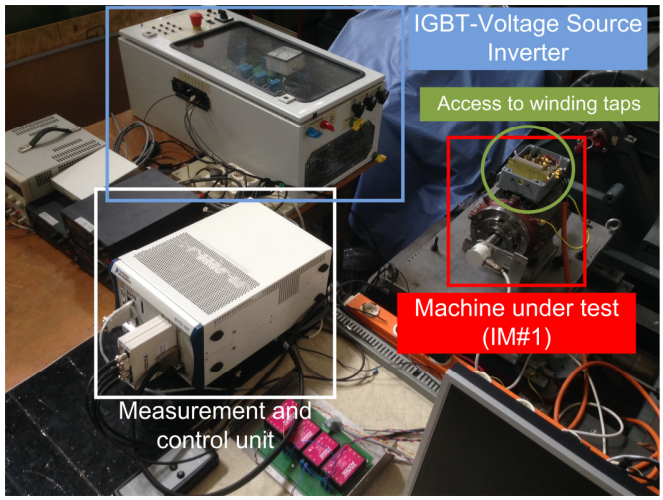

Fig. 6. Overview of used laboratory test-stand.

IV. Measurement Results

The purpose of the following experimental investigations is to identify differences in the application of the above presented monitoring method between induction machines with different power ratings and insulation systems and show

This article has been accepted for publication in a future issue of this journal, but has not been fully edited. Content may change prior to final publication. Citation information: DOI 10.1109/TIE.2014.2361114, IEEE Transactions on Industrial Electronics

the applicability of the condition monitoring method to high power machines.

In a first step the differences in the high-frequency behavior of the two investigated machines is analyzed regarding the amplitude spectrum for healthy insulation condition. Fig. 7 shows this comparison of the amplitude spectrum normalized on the respective maximum magnitude of each machine.

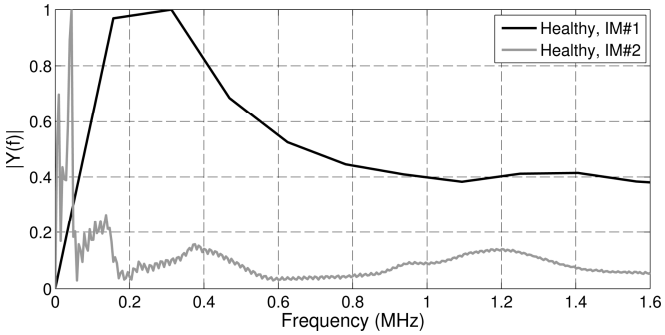

Fig. 7. Normalized Amplitude spectrum of measured current in phase U after switching transition from lower short circuit (000) to +U (001) for induction machine IM#1 (black) and IM#2 (gray).

It is clearly visible that the dominant frequencies for the machine with higher power rating (IM#2 – gray trace) are in a lower frequency range than that of IM#1 (black). The highest magnitude can be identified at 313kHz and 44kHz for induction machine IM#1 and IM#2, respectively.

The sampling rate in both investigations is chosen to 40MS/s. The investigated time window length t_{win} is defined to 6.4µs and 137.5µs for IM#1 and IM#2, respectively. The time window depends on the duration of the decaying transient oscillation visible in the current signal. The DC link voltage (voltage pulse magnitude) is in both cases 440V.

In a next investigation an additional capacitor is inserted in parallel to the full phase winding U. The value of the inserted capacitor is chosen with respect to the phase-to-ground capacitance of the two machines IM#1 (1,5nF) and IM#2 (21nF) to 0.5nF and 15nF, respectively. These values have been determined from measurements with a RLC-meter directly from the machines under test. For induction machine IM#2 further fault scenarios are evaluated too. Capacitors with a capacitance of 3nF and 6.8nF are also inserted between different taps of the stator winding (phase U). The position of the inserted capacitors has been changed. The capacitors have been inserted in parallel to the full phase winding U ('full'), first coil in phase U ('first coil') and the first turn ('first turn').

The amplitude spectra for the reference signal in phase U, $Y_{ref,U}$ (according to (3)) is compared to the amplitude during a condition measurement $|Y_{con,U,1}|$. It has to be stressed here that the condition measurement is carried out the same way as the reference measurement leading to $Y_{ref,U}$ (see detailed description section II. and [34]), however, at later time. The reference measurement is thus a characteristic finger print of the machine used to compare all later (condition) measurements. This comparison and the resulting square deviation is depicted in Fig. 8 and Fig. 9 for induction machine IM#1 and IM#2, respectively.

For both investigated machines a dominant change in specific frequency components can be detected. For IM#1 the most significant change is at 469kHz. Whereas the most dominant changes for IM#2 can be detected at 44kHz, 73kHz and 151kHz. A small deviation is detectable at 1.2MHz. This shows that the evaluation for high power machines leads to much lower frequencies. This originates in the fact of different high-frequency behavior for high-power machines (decrease of resonance frequency; see also [40]).

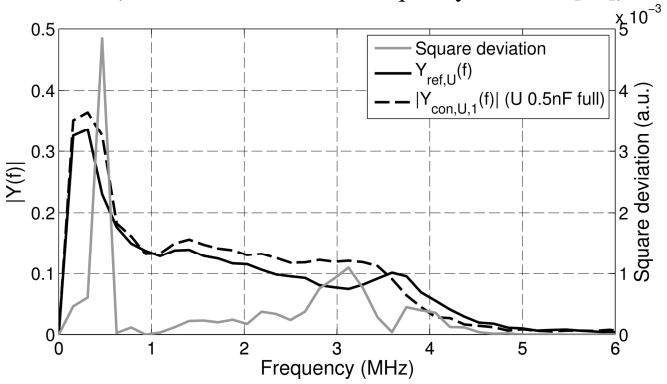

Fig. 8. Reference amplitude spectrum $Y_{ref,U}(f)$ (black, solid trace), amplitude spectrum of one condition assessment $Y_{con,U,1}(f)$ (black, dashed trace) for 0.5nF capacitor inserted in parallel to the full winding of phase U and calculated square deviation of both traces (gray, solid trace); IM#1.

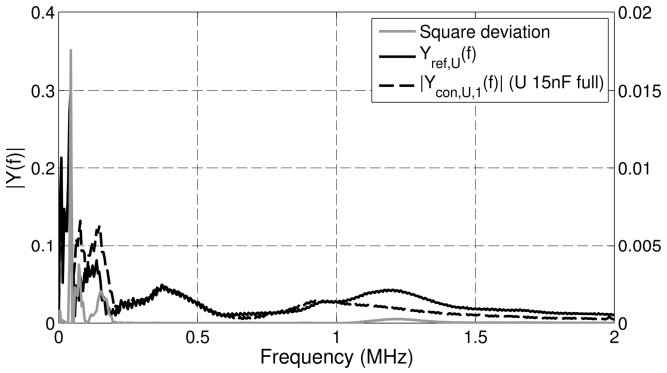

Fig. 9. Reference amplitude spectrum $Y_{ref,U}(f)$ (black, solid trace), amplitude spectrum of one condition assessment $Y_{con,U,1}(f)$ (black, dashed trace) for 15nF capacitor inserted in parallel to the full winding of phase U and calculated square deviation of both traces (gray, solid trace); IM#2.

The three most dominant changes for induction machine IM#2 are visible more clearly in Fig. 10 (zoomed plot of Fig. 9).

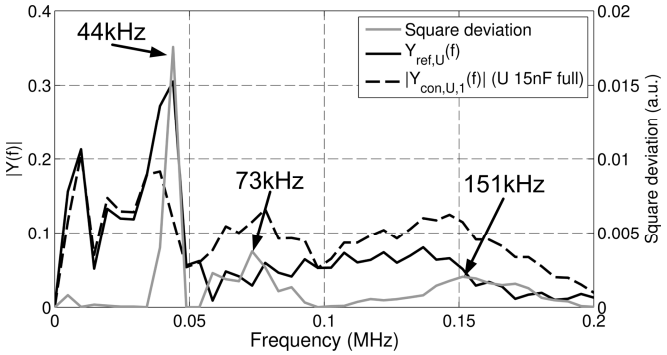

Fig. 10. Reference amplitude spectrum $Y_{ref,U}(f)$ (black, solid trace), amplitude spectrum of one condition assessment $Y_{con,U,1}(f)$ (black, dashed trace) for 15nF capacitor inserted in parallel to the full winding of phase U and calculated square deviation of both traces (gray, solid trace); IM#2 (zoomed).

The above presented comparison can be used for the calculation of the insulation state indicator for the individual phases according to equations (2), (3) and (5). The three insulation state indicators are then combined to the spatial insulation state indicator SISI according to equation (6). The frequency range taken into account for the calculation of the SISI for high power machine IM#2 is between 0Hz and

This article has been accepted for publication in a future issue of this journal, but has not been fully edited. Content may change prior to final publication. Citation information: DOI 10.1109/TIE.2014.2361114, IEEE Transactions on Industrial Electronics

200kHz (0Hz – 1MHz for IM#1). The resulting spatial representation of the indicator for induction machine IM#2 is depicted in Fig. 11.

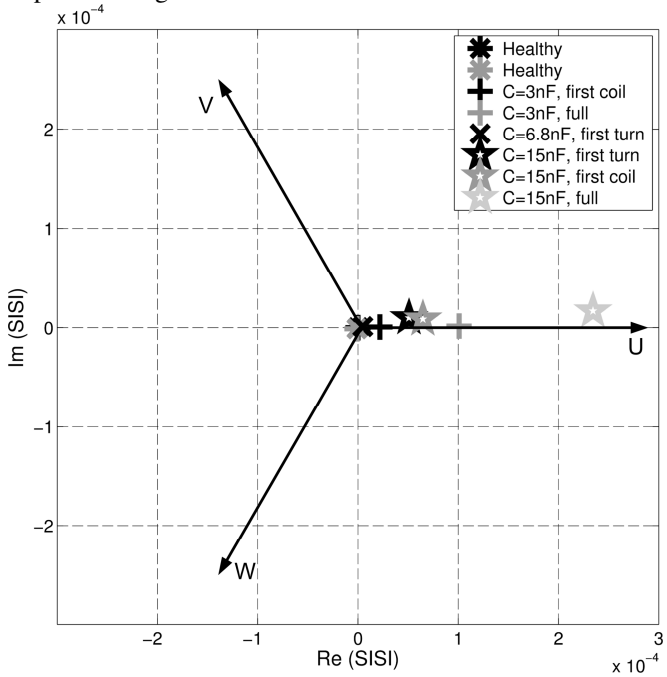

Fig. 11. Spatial insulation state indicator (SISI) for induction machine IM#2 and changed hf-behavior; sampling rate: 40MS/s.

It can be seen, that the indicator points in the direction of phase U as the change of the machine's high frequency behavior has been carried out in phase U only. The crosses, stars, etc. depict the tip of the spatial insulation state indicator. The magnitude of the spatial insulation state indicator, thus, corresponds to the severity of the alteration in the machine's hf-properties. The investigated scenarios are the ones explained above.

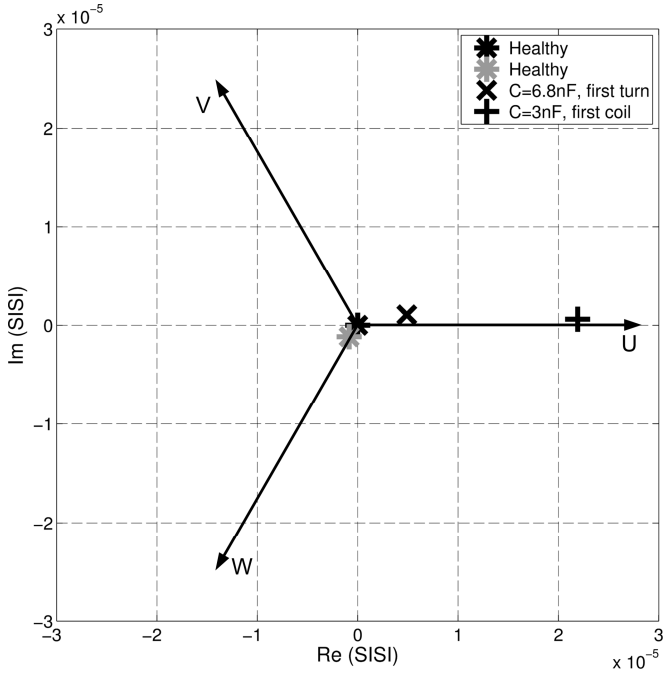

Fig. 12. Spatial insulation state indicator (SISI) for induction machine IM#2 and changed hf-behavior; sampling rate: 40MS/s (zoomed).

In Fig. 11 the spatial insulation state indicators for small changes (6.8nF capacitor across one single turn ('first turn'; black X) and 3nF across one single coil ('first coil'; black cross)) are hard to evaluate thus this area has been zoomed for better assessment of the indicator's performance. This can be seen in Fig. 12. Furthermore, it is clearly visible that the investigated healthy machine condition (black and gray star) result in a spatial insulation state indicator very close to the origin.

The results depicted in Fig. 11 and Fig. 12 show that the investigated scenarios with different severity of emulated insulation deterioration by insertion of an additional capacitor can be separated in severity by the length, the phase position of the alteration by orientation of the indicator (crosses, stars, etc. show the tip of the spatial insulation state indicator). All indicators for scenarios with changed machine's hf-properties point in phase direction U as all changes have been carried out in the respective phase. Alteration of the machine's hf-behavior introduced in phase V or W would result in an indicator with an angle of 120° and 240°, respectively. Furthermore, it can be clearly seen that unchanged machine condition always results in a spatial insulations state indicator in or close to the origin of the Gaussian plane. An indicator deviating from this position can be interpreted as an asymmetric change in the machine's hf-properties. Symmetrical changes in all three phases would not be indicated by the SISI. These changes could be introduced by change of cabling or similar aging in all three phases. However, investigations in [41] showed that insulation deterioration is usually more distinct in one of the phases. If symmetrical changes have to be considered too, the trend over time of the individual insulation state indicators (ISI) of all three phases has to be regarded in addition to the SISI.

The presented results are based on current measurements with a sampling rate of 40MS/s. In a typical control system for traction drives this sampling rate cannot be reached. For economic and also technical reasons it is thus advantageous to reduce the necessary sampling rate as much as possible. The economic reason for a reduction of sampling rate is obvious but also integration of the method into existing motor converter control systems is simplified with a reduction of necessary sampling rate. In addition to that the technical realization of high sampling rates on the one hand and real time processing of the obtained signals on the other hand is a technical challenge in the design of control electronics. This is another reason for a reduction of sampling rate as much as possible. From previous experimental investigations presented in [34] a rule of thumb could be defined saying that the necessary sampling rate for an accurate detection of a change in the machine's hf-behavior should be 20-times higher than the highest interesting frequency in the amplitude spectrum. As has been shown in Fig. 9 and Fig. 10 this frequency can be detected at 151kHz for IM#2. This results in a necessary sampling rate of around 3MS/s. Therefore the same investigations as presented in the previous figures have been performed with a sampling rate reduced from 40MS/s down to 2.6MS/s. This is even slightly below the recommended sampling rate. The results for the spatial insulation state indicator SISI investigating the same scenarios as presented in Fig. 12 for reduced sampling rate are presented in Fig. 13.

Again the indicators for small changes in the machine's hf-properties cannot be distinguished from measurements for healthy machine condition in the plot presented in Fig. 13. Thus, this area has been zoomed by a factor of ten in Fig. 14.

This article has been accepted for publication in a future issue of this journal, but has not been fully edited. Content may change prior to final publication. Citation information: DOI 10.1109/TIE.2014.2361114, IEEE Transactions on Industrial Electronics

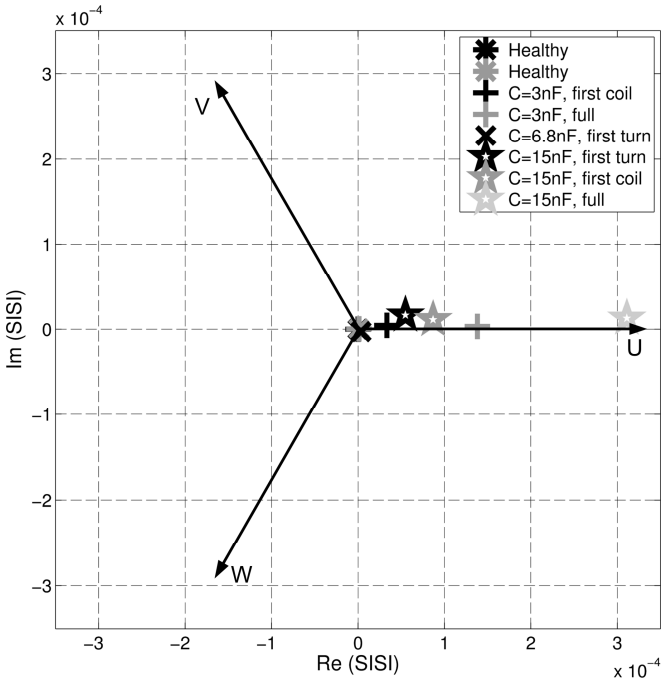

Fig. 13. Spatial insulation state indicator (SISI) for induction machine IM#2 and changed hf-behavior; sampling rate: 2.6MS/s.

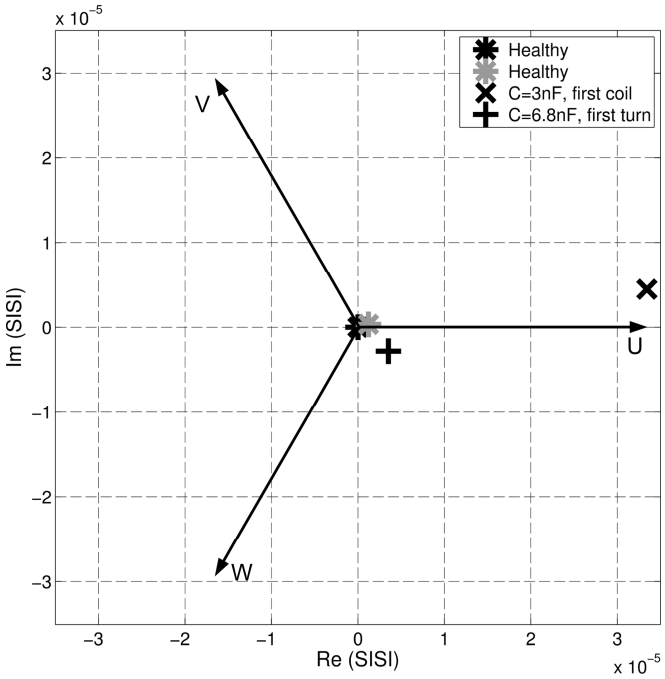

Fig. 14. Spatial insulation state indicator (SISI) for induction machine IM#2 and changed hf-behavior; sampling rate: 2.6MS/s (zoomed).

The investigations with reduced sampling rate show that similar results can be achieved as for a sampling rate of 40MS/s. The different scenarios can be identified and separated in severity and phase location. Thus, a reduction of the sampling rate to 2.6MS/s (IM#2) according to the mentioned rule of thumb is possible with hardly any deterioration in accuracy. This shows that the method can be implemented in modern drive control units with no or only minor changes in hardware.

In a last investigation the Spatial Insulation State Indicator for the low power (IM#1) and high power induction machine is analyzed. The compared scenarios are an insertion of a 0.5nF capacitor for IM#1 and a 15nF capacitor for IM#2 – both in parallel to the full phase winding. The different choice of capacitor value has to be done due to the fact that the parasitic capacitances increase for higher power machine due to the difference in insulation material and thickness (also determined by the difference in voltage rating). The results are depicted in Fig. 15.

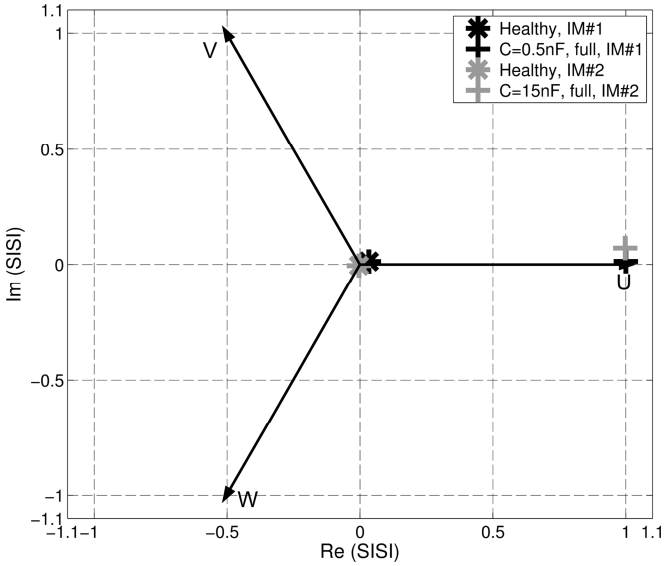

Fig. 15. Spatial insulation state indicator (SISI) for induction machine IM#1 and IM#2 and changed hf-behavior for similar scenarios.

It has to be stated here, that the SISIs have been normalized to the length of the indicator in case of additional capacitance insertion. The direct comparison of machines with different power rating is difficult due to the difference in used insulation materials and resulting parasitic capacitances. The introduced change in high-frequency behavior for IM#1 set in comparison to the machines phase-to-ground capacitances is half of that for IM#2. This leads also to a higher deviation of the healthy machine condition from origin in case of machine IM#1. The SISI calculation comparing to identical measurements would lead to an indicator exactly in the origin. Thus, the length of the indicator at healthy machine condition can be a measure for the methods performance and comparison of the two machines with different power rating. The length of the SISI indicator at healthy machine condition for IM#2 is 0.0062 and for IM#1 0.0355 and thus approximately 5.7-times higher. Comparing this value to the introduced change (2-times higher for IM#2) shows that the performance of detecting changes in the machine's hf-behavior is even better for the high power induction machine IM#2 but definitely sufficient for machines in different power ranges and with different insulation materials.

V. Conclusions

Insulation deterioration is involved in a change of the parasitic insulation capacitance. Thus, also the machine's high-frequency behavior is influenced. In this paper, a condition monitoring method has been presented that is capable of detecting such changes by evaluation of the transient current reaction resulting from a voltage step excitation immediately after inverter switching. The method has been applied to a small 5.5kW and a bigger 1.4MW induction machine having different insulation systems. The method's performance and applicability has been proven for different machine ratings and winding systems like random wound winding and pre-formed coils.

Sampling rate used for current acquisition is a crucial

parameter in the design of the measurement hardware needed. An analysis of the necessary sampling rate has been carried out and compared to previous results. The sampling rate has to be approximately 20-times higher than the maximum frequency component that experiences a significant change and is used as the upper limit in the calculation of the insulation state indicator. A sampling rate of 2.6MS/s was found to be sufficient for the investigated induction machine with a power rating of 1.4MW. An implementation of the proposed insulation condition monitoring method is thus possible with no or only minor changes in the existing hardware of modern converter control electronics.

Applying the proposed method during the operation of an industrial drive, critical changes in the insulation health state can be detected and on time repair be arranged thus reducing the risk of unpredicted sudden drive breakdown.

Due to the fact that laboratory broad-band current sensors were used for the presented investigations, an open topic for further investigations is the applicability of different types of current sensors to the method.

APPENDIX

Machine parameters:

	IM#1	IM#2
Nominal current:	14.07 A	429 A
Nominal voltage:	280 V	2183 V
Nominal frequency:	75 Hz	61.9 Hz
Rated power:	5.5 kW	1428 kW
	2-poles	4-poles

ACKNOWLEDGMENT

The authors want to thank Bombardier Transportation (Switzerland) Ltd. (GSC/PPC-CoE2, head M. Joerg and his team) and Bombardier Transportation Austria GmbH (GSC/PPC – NDEW/Drives, electrical calculation group) for their generous support. Furthermore, the authors want to thank Dr. Christoph Kehl (GSC/PPC – Chief engineer) for his generous support and all the feedback as project supervisor for several years. Special thanks from the authors also go to Mr. D. Baro (GSC/PPC-Drives Global Engineering Head) as well as Product Development GSC/PPC Drives (M. Bazant) for PDev funding and the great support.

Further thanks go to Mr. C. Zöller from TU-Vienna and the colleagues from Bombardier Transportation GSC/PPC (Mr. J. Bellingen, Mr. W. Cepak, Mrs. F. Meier, Mr. T. Nassen, Mr. R. Brammer, Mr. J. Holmberg).

Thanks also go to LEM - Company (especially Mr. W. Teppan), National Instruments Austria (Mr. G. Stefan) and ISOVOLTA - Company (especially Mr. W. Grubelnik) for the cooperation.

REFERENCES

[1] IEEE Committee Report; "Report of large motor reliability survey of industrial and commercial installation, Part I," *IEEE Trans. on Ind. Appl.,* vol.21, no.4, pp.853–864, 1985.

[2] IEEE Committee Report; "Report of large motor reliability survey of industrial and commercial installation, Part II," *IEEE Trans. on Ind. Appl.,* vol.21, no.4, pp.865–872, 1985.

[3] Nandi, S.; Toliyat, H.A.; Xiaodong Li; "Condition monitoring and fault diagnosis of electrical motors-a review," *IEEE Trans. on En. Conv.,* vol.20, no.4, pp.719-729, 2005.

[4] Bellini, A.; Filippetti, F.; Tassoni, C.; Capolino, G.-A.; "Advances in Diagnostic Techniques for Induction Machines," *IEEE Trans. on Ind. Electron.,* vol.55, no.12, pp.4109-4126, 2008.

[5] Stone, G.C.; "Advancements during the past quarter century in on-line monitoring of motor and generator winding insulation," *IEEE Trans. on Diel. and El. Ins.,* vol.9, no.5, pp.746-751, 2002.

[6] Stone, G.C.; "Recent important changes in IEEE motor and generator winding insulation diagnostic testing standards," *IEEE Trans. on Ind. Appl.,* vol.41, no.1, pp. 91-100, 2005.

[7] Guastavino, F.; Dardano, A.; Torello, E.; Massa, G. F.; "PD activity inside random wire wound motor stator insulation and early failures: A case study analysis," *in Proc. IEEE-SDEMPED,* pp.283-287, 2011.

[8] Yang, J; Cho, J.; Lee, S.B.; Yoo, J.-Y.; Kim, H.D.; "An Advanced Stator Winding Insulation Quality Assessment Technique for Inverter-Fed Machines," *IEEE Trans. on Ind. Appl.,* vol.44, no.2, pp.555-564, 2008.

[9] Stone, G.C.; Boulter, E.A.; Culbert, I.; Dhirani, H.; "Electrical Insulation for Rotating Machines," IEEE Press, Wiley & Sons, 2004.

[10] Grubic, S.; Aller, J.M.; Bin Lu; Habetler, T.G.; "A Survey on Testing and Monitoring Methods for Stator Insulation Systems of Low-Voltage Induction Machines Focusing on Turn Insulation Problems," *IEEE Trans. on Ind. Electron.,* vol.55, no.12, pp.4127-4136, 2008.

[11] Lahoud, N.; Faucher, J.; Malec, D.; Maussion, P.; "Electrical Aging of the Insulation of Low-Voltage Machines: Model Definition and Test With the Design of Experiments," *IEEE Trans. on Ind. Electron.,* vol.60, no.9, pp.4147-4155, 2013.

[12] Lahoud, N.; Faucher, J.; Malec, D.; Maussion, P.; "Electrical ageing modeling of the insulation of low voltage rotating machines fed by inverters with the design of experiments (DoE) method," *in Proc. IEEE-SDEMPED,* pp.272-277, 2011.

[13] Kaufhold, M.; Aninger, H.; Berth, M.; Speck, J.; Eberhardt, M., "Electrical stress and failure mechanism of the winding insulation in PWM-inverter-fed low-voltage induction motors," *IEEE Trans. on Ind. Electron.,* vol.47, no.2, pp.396-402, 2000.

[14] Toma, S.; Capocchi, L.; Capolino, G.-A.; "Wound-Rotor Induction Generator Inter-Turn Short-Circuits Diagnosis Using a New Digital Neural Network," *IEEE Trans. on Ind. Electron.,* vol.60, no.9, pp.4043-4052, 2013.

[15] Capocchi, L.; Toma, S.; Capolino, G.-A.; Fnaiech, F.; Yazidi, A.; "Wound-rotor induction generator short-circuit fault classification using a new neural network based on digital data," *in Proc. IEEE-SDEMPED,* pp.638-644, 2011.

[16] Ballal, M.S.; Khan, Z.J.; Suryawanshi, H.M.; Sonolikar, R.L.; "Adaptive Neural Fuzzy Inference System for the Detection of Inter-Turn Insulation and Bearing Wear Faults in Induction Motor," *IEEE Trans. on Ind. Electron.,* vol.54, no.1, pp.250-258, 2007.

[17] Sarikhani, A.; Mohammed, O.A.; "Inter-Turn Fault Detection in PM Synchronous Machines by Physics-Based Back Electromotive Force Estimation," *IEEE Trans. on Ind. Electron.,* vol.60, no.8, pp.3472-3484, 2013.

[18] Sarikhani, A.; Mirafzal, B.; Mohammed, O.; "Inter-turn fault diagnosis of PM synchronous generator for variable speed wind applications using floating-space-vector," *in Proc. IEEE-IECON,* pp.2628-2633, 2010.

[19] Siwei Cheng; Habetler, T.G.; "Using Only the DC Current Information to Detect Stator Turn Faults in Automotive Claw-Pole Generators," *IEEE Trans. on Ind. Electron.,* vol.60, no.8, pp.3462-3471, 2013.

[20] Siwei Cheng; Pinjia Zhang; Habetler, T.G.; "An Impedance Identification Approach to Sensitive Detection and Location of Stator Turn-to-Turn Faults in a Closed-Loop Multiple-Motor Drive," *IEEE Trans. on Ind. Electron.,* vol.58, no.5, pp.1545-1554, 2011.

[21] Siwei Cheng; Habetler, T.G.; "A new method to detect stator turn-to-turn faults in a closed-loop multiple-motor drive system," *in Proc. IEEE-SDEMPED.* pp.1-6, 2009.

[22] Kyeong-Hwa Kim; "Simple Online Fault Detecting Scheme for Short-Circuited Turn in a PMSM Through Current Harmonic Monitoring," *IEEE Trans. on Ind. Electron.,* vol.58, no.6, pp.2565-2568, 2011.

[23] Wiedenbrug, E.; Frey, G.; Wilson, J.; "Impulse testing and turn insulation deterioration in electric motors," *in Proc. IEEE Ann. Pulp and Paper Ind. Techn. Conf.,* pp. 50- 55, 2003.

[24] Schump, D.E.; "Testing to assure reliable operation of electric motors," *in Proc. IEEE Ind. Appl. Society Ann. Petroleum and Chemical Ind. Conf.,* pp.179-184, 1990.

[25] Stone, G.C.; Sedding, H.G.; Costello, M.J.; "Application of partial discharge testing to motor and generator stator winding maintenance," *IEEE Trans. on Ind. Appl.,* vol.32, no.2, pp.459-464, 1996.<

[26] Kheirmand, A.; Leijon, M.; Gubanski, S.M.; "New practices for partial discharge detection and localization in large rotating machines," *IEEE Trans. on Diel. and El. Ins.,* vol.10, no.6, pp.1042-1052, 2003.

This article has been accepted for publication in a future issue of this journal, but has not been fully edited. Content may change prior to final publication. Citation information: DOI 10.1109/TIE.2014.2361114, IEEE Transactions on Industrial Electronics

[27] Nelson, J.K.; Azizi-Ghannad, S.; "Measures and technologies to enhance the insulation condition monitoring of large electrical machines," *IEEE Trans. on Diel. and El. Ins.,* vol.11, no.1, pp.102-112, 2004.

[28] Jinkyu Yang; Tae-june Kang; Byunghwan Kim; Sang-Bin Lee; Young-Woo Yoon; Dongsik Kang; Jintae Cho; Heedong Kim, "Experimental evaluation of using the surge PD test as a predictive maintenance tool for monitoring turn insulation quality in random wound AC motor stator windings," *IEEE Trans. on Diel. and El. Ins.,* vol.19, no.1, pp.53-60, 2012.

[29] Younsi, K.; Neti, P.; Shah, M.; Zhou, J.Y.; Krahn, J.; Weeber, Konrad; Whitefield, C.D.; "On-line capacitance and dissipation factor monitoring of AC stator insulation," *IEEE Trans. on Diel. and El. Ins.,* vol.17, no.5, pp.1441-1452, 2010.

[30] Sang-Bin Lee; Jinkyu Yang; Younsi, K.; Bharadwaj, R.M., "An online groundwall and phase-to-phase insulation quality assessment technique for AC-machine stator windings," *IEEE Trans. on Ind. Appl.,* vol.42, no.4, pp.946-957, 2006.

[31] Jinkyu Yang; Jintae Cho; Sang-Bin Lee; Ji-Yoon Yoo; Hee Dong Kim; "An Advanced Stator Winding Insulation Quality Assessment Technique for Inverter-Fed Machines," *IEEE Trans. on Ind. Appl.,* vol.44, no.2, pp.555-564, 2008.

[32] Grubic, S.; Habetler, T.G.; Restrepo, J.; "A new concept for online surge testing for the detection of winding insulation deterioration," *in Proc. IEEE-ECCE,* pp.2747-2754, 2010.

[33] Grubic, S.; Restrepo, J.; Habetler, T.G.; "Online Surge Testing Applied to an Induction Machine With Emulated Insulation Breakdown," *IEEE Trans. on Ind. Appl.,* vol.49, no.3, pp.1358-1366, 2013.

[34] Nussbaumer, P.; Vogelsberger, M.A.; Wolbank, T.M.; "Exploitation of Induction Machine's High-Frequency Behavior for Online Insulation Monitoring," *in Proc. IEEE -SDEMPED,* pp.525-531, 2013.

[35] Kerkman, R.J.; Leggate, D.; Skibinski, G.L.; "Interaction of drive modulation and cable parameters on AC motor transients," *IEEE Trans. on Ind. Appl.,* vol. 33, pp. 722-731, 1997.

[36] Peroutka, Z. and Kus, V.; "Adverse effects in voltage source inverter-fed drive systems," *in Proc. IEEE-APEC,* pp. 557-563, 2002.

[37] Nussbaumer, P.; Wolbank, T.M.; Vogelsberger, M.A.; "Separation of disturbing influences on induction machine's high-frequency behavior to ensure accurate insulation condition monitoring," *in Proc. IEEE-APEC,* pp.1158-1163, 2013.

[38] Perisse, F.; Mercier, D.; Lefevre, E.; Roger, D.; "Robust diagnostics of stator insulation based on high frequency resonances measurements," *IEEE Trans. on Diel. and El. Ins.,* vol.16, no.5, pp.1496-1502, 2009.

[39] Savin, S.; Ait-Amar, S.; Roger, D.; "Turn-to-turn capacitance variations correlated to PDIV for AC motors monitoring," *IEEE Trans. on Diel. and El. Ins.,* vol.20, no.1, pp.34-41, 2013.

[40] Mihaila, V.; Duchesne, S. and Roger, D.; "A simulation method to predict the turn-to-turn voltage spikes in a PWM fed motor winding," *IEEE Trans. on Diel. and El. Ins.,* vol. 18, pp. 1609-1615, 2011.

[41] Farahani, M.; Gockenbach, E.; Borsi, H.; Schäfer, K.; Kaufhold, M.; "Behavior of machine insulation systems subjected to accelerated thermal aging test," *IEEE Trans. on Diel. and El. Ins.,* vol.17, no.5, pp.1364-1372, 2010.

Peter Nussbaumer (M'11) received the MSc degree in Power Engineering and the PhD. degree in Electrical Engineering from Vienna University of Technology, Vienna, Austria in 2009 and 2013, respectively.

He had been a Project Assistant at the Institute of Energy Systems and Electrical Drives, Vienna University of Technology, where he had been engaged in several industrial and scientific projects with focus on electrical drives and electric mobility. His special fields of interest are fault detection, condition monitoring and sensorless control of inverter-fed AC machines.

In 2014 he joined Bombardier Transportation, Zurich, Switzerland in the Converter Control Department as a control engineer for motor converter control of High Power Propulsion systems.

Markus A. Vogelsberger received the Dipl.-Ing. (with honor) and Dr.Techn/PhD. (with honor) degrees in Electrical Engineering from Vienna University of Technology, Vienna, Austria, in 2004 and 2009, respectively. He has been a scientific research assistant at the Institute of Electrical Drives and Machines, TU-Vienna, where he has been engaged in several industrial and scientific R&D projects.

He joined Georgia Institute of Technology University, Atlanta/USA for study and research activities in 2006 and 2008, respectively. Since 2011, he is with Bombardier Transportation, Vienna, Austria, as a Development Engineer and R&D Project lead in PPC-Drives Department.

His fields of interest include traction motors, power electronics, drives topics and multidisciplinary R&D-Projects.

In particular, currently his focus as responsible R&D-Project Lead for Drives is on the research and managing of the high innovative condition monitoring strategy (OIM) for ac traction drives and on the interdisciplinary & multi objective R&D-Project thermo efficient traction.

Thomas M. Wolbank (M'99) received the doctoral degree and the habilitation from Vienna University of Technology, Vienna, Austria, in 1996 and 2004, respectively.

Currently, he is with the Department of Energy Systems and Electrical Drives, Vienna University of Technology, Vienna, Austria.

He has coauthored more than 100 papers in refereed journals and international conferences.

His research interests include saliency based sensorless control of ac drives, dynamic properties and condition monitoring of inverter-fed machines, transient electrical behavior of ac machines, and motor drives and their components and controlling them by the use of intelligent control algorithms.